7

Emission spectroscopy for characterizing metal-halide lamps

Abstract.
The metal-halide (MH) lamp shows an unwanted axial non-uniform distribution of the metal additives when burning in the vertical position, which is caused by the interplay between convection and diffusion. Various MH lamps are investigated by means of emission spectroscopy under varying gravity conditions (1–10g) in a centrifuge. The method yields spectra, axial inhomogeneity parameters and axially integrated intensities. The method is easier than methods used before on the same type of lamp. Measurements on lamps with DyI_3 as salt filling are used as a calibration of the setup. After comparison with the earlier measurements, we conclude that the new emission spectroscopy is valid for characterization of MH lamps. Next, we apply the method on commercial lamps (Philips MASTER CosmoWhite). For these lamps, in addition NaI densities at the wall and axial temperature profiles are obtained by using self-reversed lines of Na and Hg, respectively.

This chapter has been adapted from [A.J. Flikweert, T. Nimalasuriya, G.M.W. Kroesen, M. Haverlag and W.W. Stoffels, *Emission spectroscopy for characterizing metal-halide lamps*, J. Phys. D: Appl. Phys. **41** (2008) issue 18].

7.1 Introduction

In this chapter we present results from emission spectroscopy measurements for characterizing MH lamps. The measurement technique is an addition to imaging laser absorption spectroscopy (ILAS) measurements (chapter 4) and absolute line intensity (ALI) measurements performed on the same type of lamp before [34, 37] and x-ray absorption spectroscopy measurements performed by Nimalasuriya *et al* [77] on commercial lamps, which derive absolute number densities and other plasma parameters. The emission spectroscopy method used in this chapter is easier than ILAS, ALI and x-ray absorption spectroscopy and can be used to characterize commercially available lamps.

The MH lamp is a high intensity discharge lamp with a good colour rendering index of ∼80 and a high luminous efficacy of about 100 lm W^{-1} [2, 3, 21–26, 35, 39, 42]. The lamp is used in street lighting, stadium lighting, city beautification and shop lighting.

The lamp contains a buffer gas (usually Hg) and a mixture of metal additives dosed as MH salts. The additives improve the colour rendering of the lamp. Additives that we use are DyI_3 and the filling for commercial lamps (Philips MASTER CosmoWhite: iodides of Ca, Ce, Tl, Na) [78]. When the lamp is burning in the vertical position, axial segregation of the salt additives occurs. The non-uniform light output caused by axial segregation limits the application, because it has a bad influence on the efficiency and the colour rendering of the lamp. The non-uniform distribution of additives is caused by the combination of convection and diffusion in the lamp.

The axial segregation of the additives has been described by E. Fischer [28]. The model assumes an exponential decrease of the axial Dy density n_{Dy} with increasing height z in the lamp $n_{\mathrm{Dy}}(z) \sim \exp(-\lambda z)$. The amount of axial segregation λ as a function of the ratio between the convection and diffusion speeds is shown in figure 7.1. The Fischer model is valid for infinitely long lamps with a constant axial temperature profile only. This is not the case for our lamps and therefore a semi-empirical extended model has been proposed for our lamps in chapter 5 [73]. The model takes the temperature gradient along the lamp axis into account and is valid for atomic Dy, whereas the Fischer model is valid for the elemental Dy density. Changing the temperature changes the chemical equilibrium between atoms and molecules. We use the axial inhomogeneity parameter α, which can be used to describe any axial non-uniformity in a lamp. In our case we want to describe the non-uniformity of emission and use it to describe the axial intensity inhomogeneity of several emission peaks.

Convection is induced by gravity. In the past several experiments under varying gravity conditions have been carried out. Beside lab experiments (chapter 2, [32, 34, 35, 50]), the lamp was sent to the International Space Station (micro-gravity $0g$; in this chapter the amount of acceleration is given in terms of $g = 9.81$ m s^{-2}) [41]. Furthermore parabolic flights were carried out (0–2g, for periods of about 20 s; chapter 3) [33, 67]. More recently a centrifuge was built, in which we can achieve gravity conditions from 1–10g (chapters 4 and 8) [37–39]. The additive distribution in the

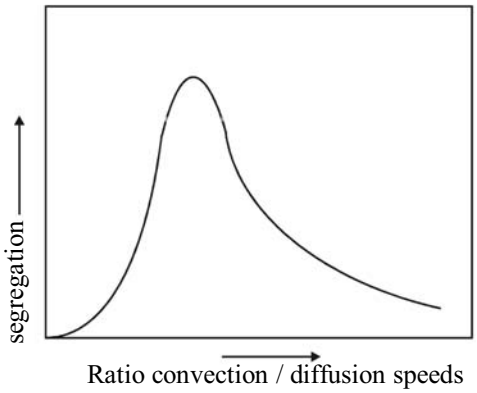

Figure 7.1: The Fischer curve shows the axial segregation as a function of the ratio between the convection and diffusion speeds [28, 32, 67, 73]. In our case the amount of convection is changed by changing the gravitational acceleration. The DyI_3 lamps we use are around the maximum of the curve.

Table 7.1: Lamp specifications. The diameter and height refer to the inner wall of the burner. The CosmoWhite salt filling consists of a mixture of Ca, Ce, Tl and Na iodides.

Lamp name	Burner material	Diameter (mm)	Height (mm)	Electrode dist. (mm)	Hg (mg)	Salt filling
Q1	Quartz	8	20	16	5	4 mg DyI_3
Q2	Quartz	8	20	16	7.5	4 mg DyI_3
Q3	Quartz	8	20	16	10	4 mg DyI_3
Q4	Quartz	8	15.5	8	6	4 mg DyI_3
Q5	Quartz	8	14	8	12	4 mg DyI_3
Q6	Quartz	4	22	16	0.7	2.5 mg DyI_3
Q7	Quartz	4	22	16	2.5	2.5 mg DyI_3
C1	PCA	5.3	26.0	23.0	2.5	CosmoWhite
C2	PCA	9.2	13.3	9.0	14.4	CosmoWhite

lamp has been measured by means of ALI measurements [34, 35, 38, 41] and ILAS (chapters 4 and 8) [37, 39, 67, 71, 72]. By using ALI absolute number densities of Dy and Hg, and temperature profiles were obtained. ILAS yields the ground state atomic Dy density distribution in the lamp. When using ALI, the setup needs to be calibrated to obtain absolute intensities. Temperatures are calculated using Boltzmann plots [31]. This method is complicated, time consuming and sensitive to errors in the transition

probabilities. The ILAS technique also yields absolute number densities, but due to the optics and the laser wavelength ILAS is limited to quartz lamps with a fixed diameter of 8 mm and DyI_3 as salt additive.

We want to have an easier, faster method to characterize MH lamps. Therefore we perform emission spectroscopy measurements on lamps that have been measured by ILAS and ALI. We validate the fast emission spectroscopy method by comparing the measurement results with the results from earlier measurements, so the emission spectroscopy can be used to characterize commercially available lamps.

In this chapter we present a method based on emission spectroscopy, which determines the axial additive inhomogeneity in the lamps in a faster way than ILAS and ALI. The setup is not only limited to the fixed diameter, the DyI_3 salt filling or the quartz burner. Lamps with different salt fillings and burner materials (quartz and poly-crystalline alumina, PCA) can be measured. This allows us to investigate also commercial lamps like the Philips MASTER CosmoWhite.

The structure of this chapter is as follows. First the setup is discussed, the lamps that are measured, the centrifuge to vary the gravity conditions, and the emission spectroscopy setup. Next, the analysis of the measurement data is discussed. We show results for the lamps with DyI_3, which are compared with results obtained by ILAS before [72]. Finally the results are shown for the commercially available Philips MASTER CosmoWhite lamp.

7.2 Experimental method

Lamps with various geometries, salt fillings and wall materials (quartz and PCA) are investigated by means of emission spectroscopy. This has been done in the centrifuge, where we can achieve gravity conditions between $1g$ and $10g$.

7.2.1 Lamps

The specifications of the lamps are given in table 7.1. The lamps all have a fitting according to the MH reference lamp developed within the European COST action program 529 [27], which is required for use of the lamps in the centrifuge setup (see also section 1.3.1). A schematic picture of the MH reference lamp is given in figure 7.2(a).

The lamps have different Hg pressures and different salt additives: DyI_3 and the commercial Philips CosmoWhite filling (iodides of Ca, Ce, Tl, Na). Lamp C1 (see table 7.1) contains the burner of the Philips MASTER CosmoWhite 140W lamp. Lamp C2 also has the CosmoWhite filling, but has a different geometry.

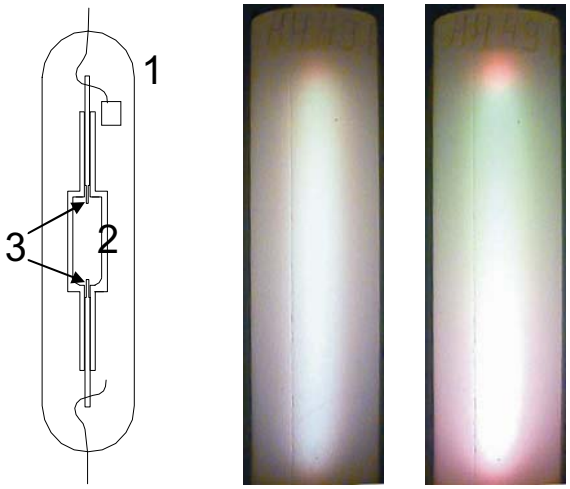

(a) MH reference lamp (b) C1 $1g$ (c) C1 $10g$

Figure 7.2: (a) Schematic drawing of the MH reference lamp [27, 37]: (1) outer bulb; (2) burner (diameter 8 mm, height between 14 and 20 mm); (3) electrodes (distance 8 or 16 mm).
(b)–(c) Webcam images of the Philips CosmoWhite lamp C1, 141.6 W at $1g$ and $10g$. The axial colour segregation is clearly seen. For this lamp, increasing the gravitational acceleration thus enhances convection, and increases the axial colour segregation. This means that the lamp is at the left-hand side in the Fischer curve in figure 7.1.

7.2.2 Centrifuge

The amount of convection in the lamps depends on gravity [33, 37–39, 41, 67, 71, 72]. A centrifuge was built to investigate the lamp under varying gravitational accelerations. The centrifuge has a diameter of about 3 m. It consists of a pivot, an arm, and a gondola connected to the arm. The gondola contains the lamp and the emission spectroscopy setup. The maximum rotation speed is $\sim$ 1.5 Hz, corresponding to $10g$ at the lamp position.

Figure 7.3 shows a drawing of the centrifuge arm with gondola. The vectors of the acceleration working on the lamp are shown; the total gravitational acceleration at the lamp $\vec{a}_{\text{tot}}$ is the vector sum of the gravity on earth $\vec{g}_z$ and the centrifugal acceleration $\vec{a}_r$. The gravity vector $\vec{a}_{\text{tot}}$ at the lamp is always parallel to the lamp axis; the size of the vector parallel to the lamp axis is defined by $|\vec{a}_{\text{tot}}| = a_z$.

Figures 7.2(b) and (c) show the effect of the gravity conditions on the axial colour segregation, for the commercial Philips CosmoWhite lamp C1.

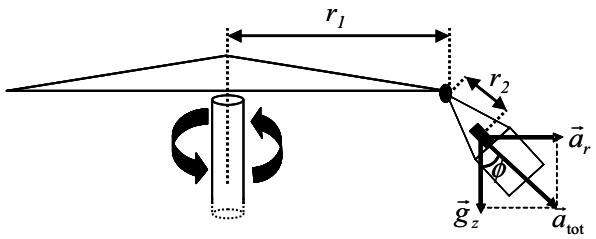

Figure 7.3: Schematic representation of the centrifuge arm with the gondola. When rotating, the gondola swings out with an angle ϕ. The acceleration vectors at the position of the lamp are indicated [37, 38, 67]. The size of the vector parallel to the lamp axis is defined by $|\vec{a}_{\mathrm{tot}}| = a_z$, which is used in the rest of this chapter.

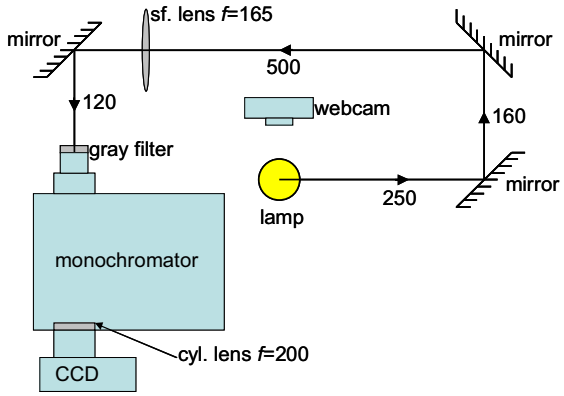

Figure 7.4: Top view of the emission setup. The lamp is focused on the entrance slit (in the vertical position) of the spectrometer. At the 2D CCD chip the wavelength is in the horizontal and the axial position of the lamp in the vertical direction. All measures are given in millimetres. The setup is mounted on the centrifuge gondola; mirrors are used to increase the path length between the lamp and entrance slit.

7.2.3 Emission spectroscopy setup

The lamps are characterized by means of emission spectroscopy. Emission spectroscopy in the centrifuge has been discussed in detail by Nimalasuriya *et al* [38]. We do not perform ALI measurements, but use the intensity of the line emission peaks (peak area) for the analyses without absolute number calibration.

The setup is shown schematically in figure 7.4. The spectrometer is a Yvon-Jobin 0.25 m monochromator. The lamp is focused on the entrance slit of the spectrometer by three mirrors and a lens. The entrance slit (width 100 μm) of the spectrometer is in the

Table 7.2: Emission lines that have been investigated.

Element	λ (nm)
Dy	642.19
Hg	546.07
Ca	442.67
Ce	556.5
Tl	535.05
Na	doublet 589.0 / 589.6

vertical direction; in this way an axial profile of the lamp is imaged on the spectrometer slit. A neutral density filter (transmission 10^{-3}) is placed in front of the slit. At the exit of the spectrometer a CCD camera (SBIG ST-2000 XM) [60] is attached. The horizontal position at the CCD camera corresponds to the wavelength and the vertical position to the axial position in the lamp. The wavelength range that can be imaged on the CCD camera is $\sim$ 30 nm. Because the spectrometer was originally not meant for imaging purposes on a 2D CCD camera, the wavelength and the axial position do not have the same focal plane at the exit of the spectrometer. To correct for this, a cylindrical lens with $f = 200$ mm is placed just before the exit of the spectrometer. In this way, the setup is aligned so the wavelength and axial focal planes are both at the position of the CCD chip. The calibration of the wavelength is done using a Hg/Ar calibration lamp. The spectral resolution of the setup is 0.02 nm per pixel and the instrumentally observed line width is $\sim$0.2 nm.

A typical image obtained by the CCD camera is shown in figure 7.5. The shutter time of the camera is set between 100 and 4000 ms, depending on the maximum peak intensity in the spectrum. At the CCD image, the wavelength is in the horizontal direction and the axial position in the lamp is in the vertical direction. A spectrum can be determined for a particular axial position, as is indicated in figure 7.5. After normalization for the shutter time and correction for the spectral response of the system by a tungsten ribbon lamp, the intensities of different spectra can be compared. For one particular wavelength, an axial intensity profile is obtained. In this example, the axial intensity profile for the 642.19 nm peak of atomic Dy is shown. This can be done for each wavelength of interest.

For the lines of interest, the integrated line intensity and the maximum intensity of the peak are determined. These values are corrected for the baseline of the background radiation. For the line intensity, the area under the peak is calculated from the range where the intensity is above 10% of the peak height. The investigated emission lines for the various lamps are shown in table 7.2. The Na doublet lines are used for the density calculation from self-reversed lines as is explained in section 7.3.2.

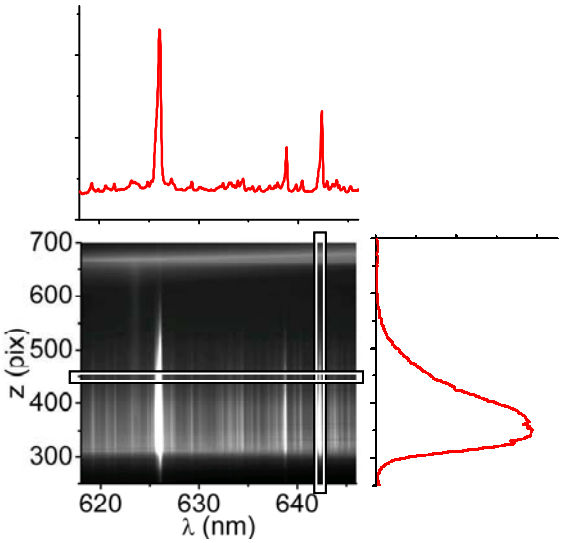

Figure 7.5: CCD image of lamp Q3 (10 mg Hg, 4 mg DyI_3), 148.4 W at $1g$. In the CCD image, the horizontal axis is the wavelength λ and the vertical axis is the axial position z in the lamp. The spectrum (top graph) is taken around $z = 450$ and in the graph at the right the intensity of the 642.19 nm peak is plotted as a function of the axial position.

The lamps are driven by a Luxmate DimTronic ballast with a square wave voltage of 120 Hz. This frequency corresponds to a period of 8.33 ms. As mentioned, the shutter time of the CCD camera is set between 100 and 4000 ms. This time is much longer than the period of the ballast, so phase dependent fluctuations are averaged out during one camera exposure.

7.3 Analysis

From the emission spectroscopy measurements, spectra are obtained for each axial position in the lamp. From these spectra, we want to determine the non-uniformity of the emission of the various lamp species over the axial position in the lamp. Hereto we introduce the axial line intensity inhomogeneity. Next, the Na density is derived for each axial position using a self-reversed Na-D line. Finally we verify an existing method to calculate the axial temperature profile by using self-reversed lines of Hg.

7.3.1 Axial line intensity inhomogeneity

We want to have a measure for the axial non-uniformity of the light output for different particles in the lamp. In section 5.3.3 [73] the inhomogeneity parameter α has been introduced. In most cases the square of the inhomogeneity (α^2) follows the same trend as the Fischer parameter, which describes the amount of axial segregation. Figure 7.1 shows the amount of axial segregation as a function of the amount of convection.

The inhomogeneity parameter describes the axial inhomogeneity of any lamp property Q. In our case $Q(z)$ denotes the line intensity (area under the peak) of a spectral line, or the density, at the axial position z. The axial inhomogeneity, which is a measure for the axial non-uniformity of property $Q(z)$, is given by

$$\alpha = \sqrt{\frac{1}{H}\int_0^H \left(\frac{Q(z)-\overline{Q}}{\overline{Q}}\right)^2 \mathrm{d}z}, \tag{7.1}$$

where H is the lamp height and $\overline{Q}$ is the averaged value of $Q(z)$ over the lamp height:

$$\overline{Q} = \frac{1}{H}\int_0^H Q(z)\mathrm{d}z. \tag{7.2}$$

7.3.2 Density calculation using self-reversed lines

From the contour of a self-reversed line of a radiating particle, the density can be calculated for that particle [79–81]. This density calculation is an empirical method.

In our case, we use the Na-D line (589.0 and 589.6 nm). The distance $\Delta\lambda_{\mathrm{Na}}$ between the maximum left λ_1 and the maximum right λ_2 of this wavelength is a measure for the Na density. Hoek *et al* [79] obtained

$$[\mathrm{NaI}]_{\mathrm{w}}(z) \propto (\Delta\lambda_{\mathrm{Na}}(z) - 0.6)^{1.43}, \tag{7.3}$$

where $[\mathrm{NaI}]_{\mathrm{w}}(z)$ is the NaI density at the wall for each axial position z, $\Delta\lambda_{\mathrm{Na}}(z) = \lambda_1 - \lambda_2$ (in nm) is the distance between the two maxima at the axial position z and 0.6 nm is the distance between the two Na-D lines. In this equation the Hg density is assumed to be independent of the axial position. The axial density distribution obtained by this equation can also be analysed by means of the inhomogeneity parameter α (equation (7.1)), where $Q(z) = [\mathrm{NaI}]_{\mathrm{w}}(z)$. In this case, the parameter α describes the axial density inhomogeneity at the wall and not at the centre of the burner. We assume that the atomic Na density at the centre of the burner follows the same trend and then α is also a measure for the axial Na density inhomogeneity at the centre.

7.3.3 Temperature calculation using self-reversed lines

The temperature can be determined using self-reversed lines. Wesselink *et al* [82] presented a variation on Bartels' method [80, 81] for determining the temperature of

Table 7.3: Parameters of the self-reversed Hg lines used to determine the temperature [44].

Peak number	λ (nm)	E_m (eV)	E_j (eV)	MY
1	435.83	4.887	7.731	0.7062
2	546.07	5.461	7.731	0.7660

an optically thick plasma. Here we want to verify this method for our lamps and setup, and want to have at least a qualitative measure for the axial temperature profile in the CosmoWhite lamp C1.

For the temperature determination using the Wesselink method, we need two self-reversed lines with wavelengths λ_1 and λ_2. The intensity (W m^{-2} sr^{-1} nm^{-1}) at the top of the first line I_{λ_1} and the intensity at the top of the second line I_{λ_2} are determined from the emission spectra. According to this method the maximum temperature T_m within the line-of-sight is given by [82]

$$T_\mathrm{m} = \frac{hc\left(\lambda_1^{-1} - \lambda_2^{-1}\right)}{k} \times \frac{1}{\ln\left(I_{\lambda_2}/I_{\lambda_1}\right) + \ln\left(Y_1 M_1 / Y_2 M_2\right) + 5\ln\left(\lambda_2/\lambda_1\right)}, \tag{7.4}$$

where h is the Planck constant, k is the Boltzmann constant, c is the speed of light, and Y_1, Y_2 and M_1, M_2 are the grayness factors of the first and second line. The values for Y and M are [80–85]

$$M_\infty = \sqrt{\frac{E_m}{E_j}} \tag{7.5}$$

and

$$Y_\infty = 0.736 + 0.264q^2, \tag{7.6}$$

where

$$q = \frac{6}{\pi}\tan^{-1}\frac{M_\infty^2}{\sqrt{1+2M_\infty^2}}. \tag{7.7}$$

In these equations E_m and E_j are the lower and upper energy level, respectively. Note that the factors in the denominator (e.g. the factor 5) in equation (7.4) are empirical; therefore the temperature T_m should be considered as a qualitative parameter. The obtained values for our lamp C1 should be used to indicate trends as a function of the axial position in the lamp and as a function of the gravitational acceleration.

In table 7.3 the values needed for the temperature calculations are given.

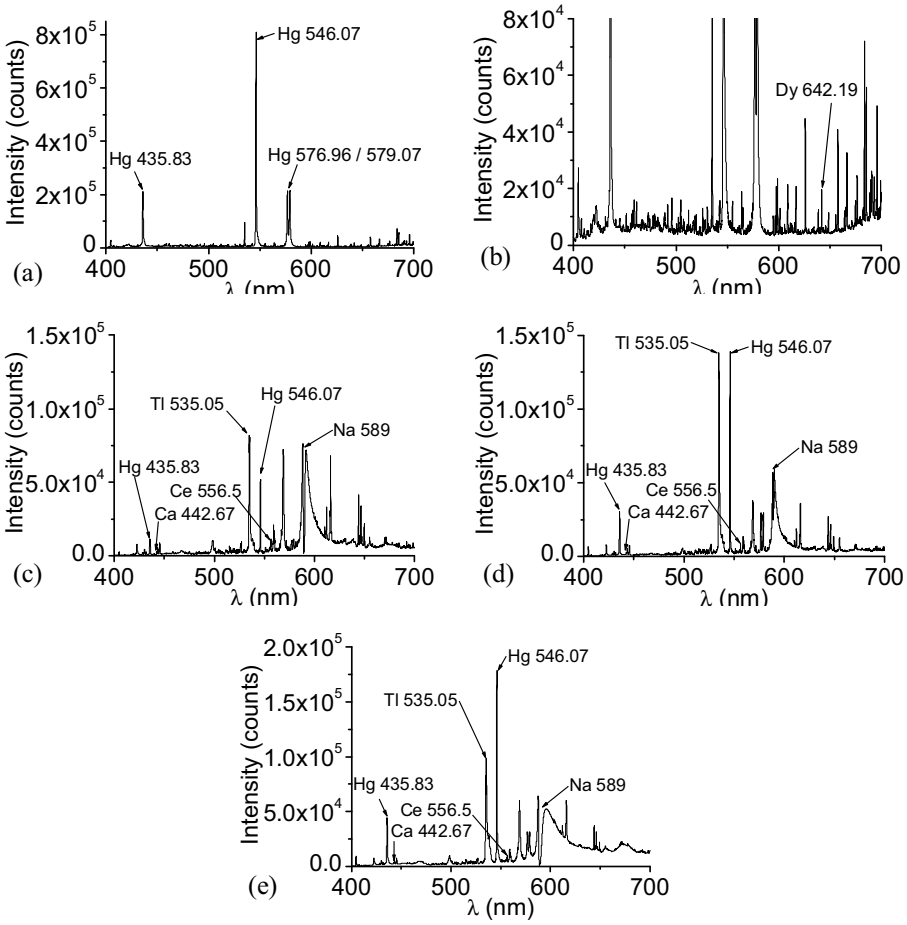

Figure 7.6: Spectra for various lamps, obtained by optical emission spectroscopy. The intensity is integrated over the lamp axis and normalized for a shutter time of 1000 ms. The main peaks are indicated (see also table 7.2). (a) 1*g*, lamp Q3 (10 mg Hg, 4 mg DyI_3), 148.4 W. (b) 1*g*, lamp Q3 (10 mg Hg, 4 mg DyI_3), 148.4 W; same spectrum as (a), with a different intensity scale to display the Dy peaks. (c) 1*g*, lamp C1 (MASTER CosmoWhite), 141.6 W. (d) 10*g*, lamp C1 (MASTER CosmoWhite), 141.6 W. (e) 1*g*, lamp C2 (CosmoWhite filling, short lamp), 148.4 W.

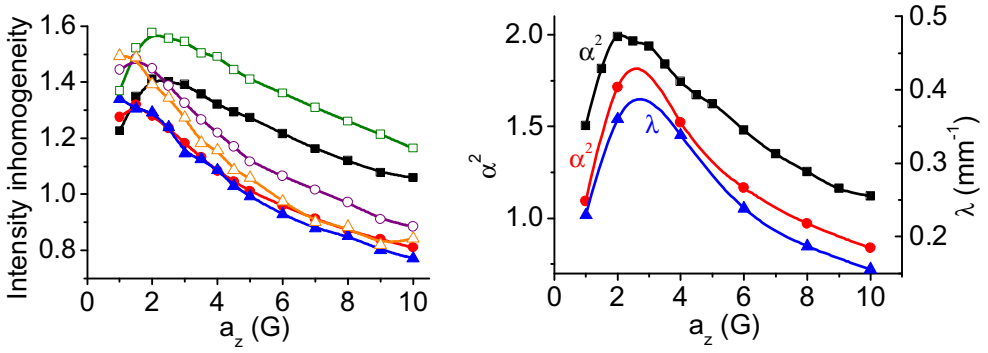

Figure 7.7: (a) Axial intensity inhomogeneity α (equation (7.1)) of Dy 642.19 nm for lamps Q1–Q3 (different Hg pressures, different input power), as a function of the gravitational acceleration a_z. The lines are shown to guide the eye: lamp Q1 (5 mg Hg) ■ 148.4 W, □ 129.9 W; lamp Q2 (7.5 mg Hg) ● 148.4 W, ○ 129.9 W; lamp Q3 (10 mg Hg) ▲ 148.4 W, △ 129.9 W.
(b) Square of the axial inhomogeneity (α^2) (equation (7.1)) and the axial segregation λ of Dy 642.19 nm for lamp Q1 (5 mg Hg, 4 mg DyI_3), 148.4 W, as a function of the gravitational acceleration a_z, comparison between emission spectroscopy, ILAS and ALI. The curves for lamps Q2 and Q3 show the same trends and are not shown for clarity [72]. ■ Emission spectroscopy (square of the intensity inhomogeneity; left axis); ● ILAS (square of the density inhomogeneity; left axis); ▲ ALI (axial segregation λ; right axis) [38].

7.4 Results

The lamps described in table 7.1 have been investigated. Some of the axially integrated spectra of these lamps, under $1g$ and $10g$, are shown in figure 7.6 and are discussed in more detail later.

First we discuss lamps with DyI_3 as salt additive. Next lamps with the commercial Philips CosmoWhite filling are discussed. In the figures a_z is the acceleration parallel to the lamp axis; the unit G is defined as 9.81 m s^{-2}.

7.4.1 Lamps with DyI_3 filling

Spectra

Various lamps with DyI_3 as salt filling have been measured. The spectrum of lamp Q3 (10 mg Hg), at $1g$, is shown in figures 7.6(a) and (b). In the second figure the intensity scale is different to display the Dy peaks. The spectra are axially integrated spectra. The Hg peaks are most pronounced in these spectra. Dy mainly stays at the bottom;

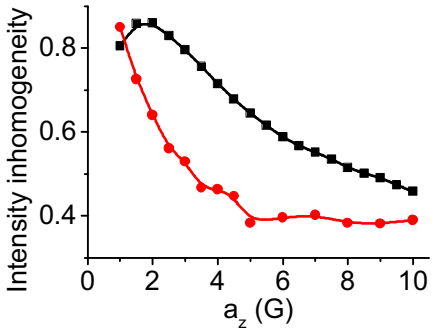

Figure 7.8: Axial intensity inhomogeneity α (equation (7.1)) of Dy 642.19 nm for lamps Q4 and Q5 (wide, short burner), as a function of the gravitational acceleration a_z: ■ lamp Q4 (6 mg Hg), 89.5 W; ● lamp Q5 (12 mg Hg), 89.5 W.

therefore the axially integrated spectra only show small Dy peaks as they appear mainly at the bottom of the lamp.

Axial intensity inhomogeneity

For the DyI_3 lamps, the values for the axial line intensity inhomogeneity α of the Dy-642 peak have been obtained (equation (7.1)) for different gravitational accelerations. The results for the lamps with quartz burner (Q1–Q3) are shown in figure 7.7(a). In all graphs, lines are shown to guide the eye. The values for the axial intensity inhomogeneity α are in agreement with the values for the density inhomogeneity obtained by ILAS in chapter 6 [72] and the results obtained by ALI [38]. This is seen in figure 7.7(b), which shows the values for the square of the axial intensity inhomogeneity (α^2) at 148.4 W for the three lamps Q1–Q3, for emission spectroscopy and ILAS, and the axial segregation λ for ALI. The shapes of the curves for the same lamp are in agreement and the positions of the maximums are found at the same gravitational acceleration. The small difference is explained by the difference in measurement technique: ILAS yields the number density of the ground state Dy atoms, whereas by emission spectroscopy the intensity of radiating Dy atoms (Dy-642) is measured. The intensity is affected by temperature stronger than the absolute number density, due to the temperature dependence of the highly excited states, causing a stronger temperature effect in the axial inhomogeneity parameter. For further explanation on the axial temperature gradient the reader is referred to chapter 5 [73].

The axial intensity inhomogeneity α of the short lamps Q4 and Q5 (containing 6 mg and 12 mg Hg, respectively) are shown in figure 7.8. For lamp Q4 (6 mg Hg) the maximum axial intensity inhomogeneity is around $2g$. Lamp Q5 contains 12 mg Hg and has therefore a higher convection speed ($v \sim p_{\mathrm{Hg}}$) [42, 53, 73], increasing the

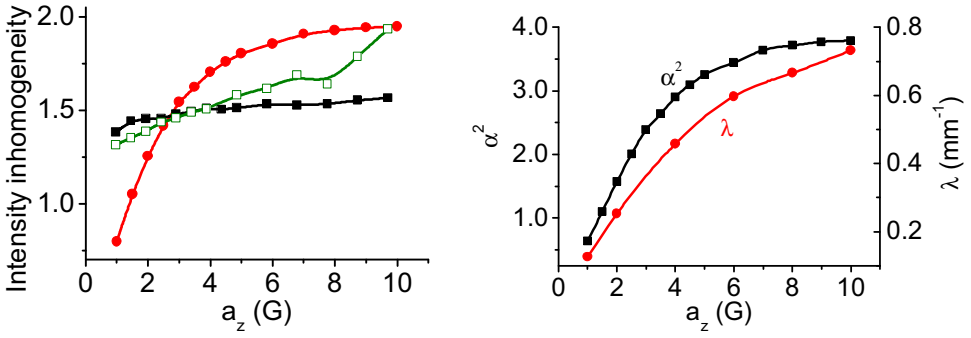

Figure 7.9: (a) Axial intensity inhomogeneity α (equation (7.1)) of Dy 642.19 nm for lamps Q6 and Q7 (thin, long burner), as a function of the gravitational acceleration a_z: ■ lamp Q6 (0.7 mg Hg) 129.9 W (values have been multiplied by 3), □ lamp Q6 101.7 W (values have been multiplied by 3), ● lamp Q7 (2.5 mg Hg) 129.9 W.
(b) Square of the axial inhomogeneity (α^2) (equation (7.1)) and the axial segregation λ of Dy 642.19 nm for lamp Q6 (0.7 mg Hg), 129.9 W, as a function of the gravitational acceleration a_z, comparison between emission spectroscopy and ALI. The curve for lamp Q7 shows the same trend and is not shown for clarity [72]. ■ Emission spectroscopy (square of the intensity inhomogeneity; left axis); ● ALI (axial segregation λ; right axis) [38].

ratio between convection and diffusion speeds. This explains that we are more at the right-hand side of the Fischer curve (figure 7.1) for this lamp Q5.

The values for α for 6 mg Hg are in agreement with the ILAS measurements [72]. Above $5g$, the axial intensity inhomogeneity α is still decreasing for emission spectroscopy, whereas α is only slightly decreasing for ILAS. For 12 mg Hg the values for α are different for emission spectroscopy and ILAS, especially above $5g$. For emission spectroscopy the axial intensity inhomogeneity is constant at $\alpha \approx 0.4$ above $5g$. For ILAS $\alpha \approx 0.4$ for $4g$, and next we observe a jump to a constant level of $\alpha \approx 0.6$ above $4g$. This difference is explained by the larger temperature effect for the 12 mg Hg lamp, compared with the 6 mg Hg lamp.

If we compare the values for α for the lamps Q4 and Q5 (figure 7.8) with those for the lamps Q1–Q3 (figure 7.7(a)), we are more at the right-hand side in the Fischer curve for lamps Q4 and Q5. This is because of the larger ratio between the radius and the height of the burner [73].

Figure 7.9(a) shows the axial intensity inhomogeneity α for the lamps with the long, thin burner Q6 and Q7. These curves show that we are at the left-hand side of the Fischer curve. The ratio between the height and radius of the burner is larger than for lamps Q1–Q5, causing a larger ratio between the convection and diffusion speeds [73]. For lamp Q6 (0.7 mg Hg) we are at the far left-hand side of the Fischer curve. We see

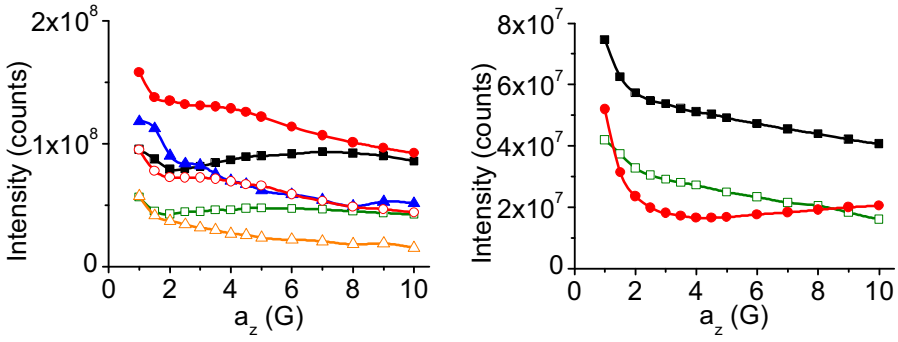

(a) (b)

Figure 7.10: (a) Axially integrated intensity of Dy 642.19 nm, as a function of the gravitational acceleration a_z, for lamps Q1–Q3. The lamps show maximum intensity at $1g$ and are therefore optimized for $1g$. Lamp Q1 (5 mg Hg) ■ 148.4 W, □ 129.9 W; lamp Q2 (7.5 mg Hg) ● 148.4 W, ○ 129.9 W; lamp Q3 (10 mg Hg) ▲ 148.4 W, △ 129.9 W.
(b) Axially integrated intensity of Dy 642.19 nm, as a function of the gravitational acceleration a_z, for lamps Q6 and Q7 (thin, long burner): ■ lamp Q6 (0.7 mg Hg) 129.9 W, □ lamp Q6 101.7 W, ● lamp Q7 (2.5 mg Hg) 129.9 W.

that the axial intensity inhomogeneity is much lower than for lamp Q7 (2.5 mg Hg) and the inhomogeneity increases with a smaller slope than lamp Q6. The values for the square of the axial intensity inhomogeneity (α^2) are in agreement with the values for the axial segregation λ obtained by ALI [38]. This is seen in figure 7.9(b), which shows these values at 129.9 W for lamp Q6 for emission spectroscopy and ALI.

The trends for the square of the axial intensity inhomogeneity parameter (α^2) for lamps Q1–Q3 and Q6 and Q7 are in agreement with the results obtained for the axial segregation parameter λ measured by ALI by Nimalasuriya *et al* [38].

From the results and the comparison with the results obtained by ILAS for lamps Q1–Q3, we conclude that the emission spectroscopy can be used to characterize MH lamps.

Axially integrated intensity

Figure 7.10(a) shows the axially integrated intensity of the atomic Dy peak at 642.19 nm as a function of the gravitational acceleration, for the quartz lamps Q1–Q3, at two different values for the input power. The maximum intensity is at $1g$, showing that the lamp was optimized for $1g$. The intensity decreases as a function of the gravitational acceleration for lamps Q2 and Q3 (7.5 and 10 mg Hg). For Q1 (5 mg Hg) the intensity first decreases. The minimum in the intensity is found at the maximum of α (figure 7.7(a)). Beyond the minimum, the intensity increases again slightly. For lower Hg

pressure a second maximum in intensity is observed.

The axially integrated intensity of Dy 642.19 nm for lamps Q6 and Q7 is shown in figure 7.10(b). The intensity for the lamps burning at 129.9 W is in the same order of magnitude as the intensity for lamps Q1–Q3 at 129.9 W. Lamps Q6 and Q7 are also optimized for $1g$. The intensity decreases rapidly when increasing the gravitational acceleration. The geometry of the lamp is important; comparing lamps Q1–Q3 with Q6 and Q7 shows different behaviour. A minimum in intensity for lamps Q6 and Q7 is found at higher Hg pressure, whereas for lamps Q1–Q3 the minimum is found at lower Hg pressure.

The comparison between ILAS and emission spectroscopy for the quartz lamps with DyI_3 shows that the intensity inhomogeneity obtained by emission is in agreement with the density inhomogeneity obtained by ILAS. Now the emission spectroscopy setup has been validated, we can also use the emission spectroscopy setup to characterize lamps with a commercial filling, which we could not investigate using ILAS.

7.4.2 Lamps with CosmoWhite filling

The burner of the commercial Philips CosmoWhite lamp (C1) has been fit into a MH reference lamp outer bulb [27], so it fits in the setup. In addition, lamp C2 has been investigated. This lamp has a shorter, wider burner than the CosmoWhite lamp, but contains the same salt mixture.

Spectra

In the spectra of lamp C1 in figures 7.6(c) and (d) we see an increase of the Tl-535 and Hg-546 peaks in comparison to the radiation from Na-589, when the gravitational acceleration is increased from $1g$ to $10g$. This is also observed by eye when looking directly at the lamp, where we see the colour of the lamp changing from orange towards yellow–green. The webcam images of lamp C1 at $1g$ and $10g$ are shown in figures 7.2(b) and (c).

The spectrum of lamp C2 is shown in figure 7.6(e). When this spectrum is compared with the spectrum of C1 (figure 7.6(c)), we see that the peaks are more broadened (especially the Na-589 line), because of the higher Hg pressure. Lamp C2 contains 12.5 mg Hg, whereas C1 contains only 2.5 mg Hg (table 7.1).

NaI density

Figure 7.11 shows spectra around the Na-D lines at 589 nm for lamp C1, for two different axial positions z, at $1g$ and $10g$. According to equation (7.3) we need $\Delta\lambda$ to calculate the NaI density at the wall. This $\Delta\lambda$ is indicated in the spectra. After calculation of these values for every axial position z in the lamp, we obtain a NaI wall density profile as a function of the axial position. Figure 7.12 shows the density profiles

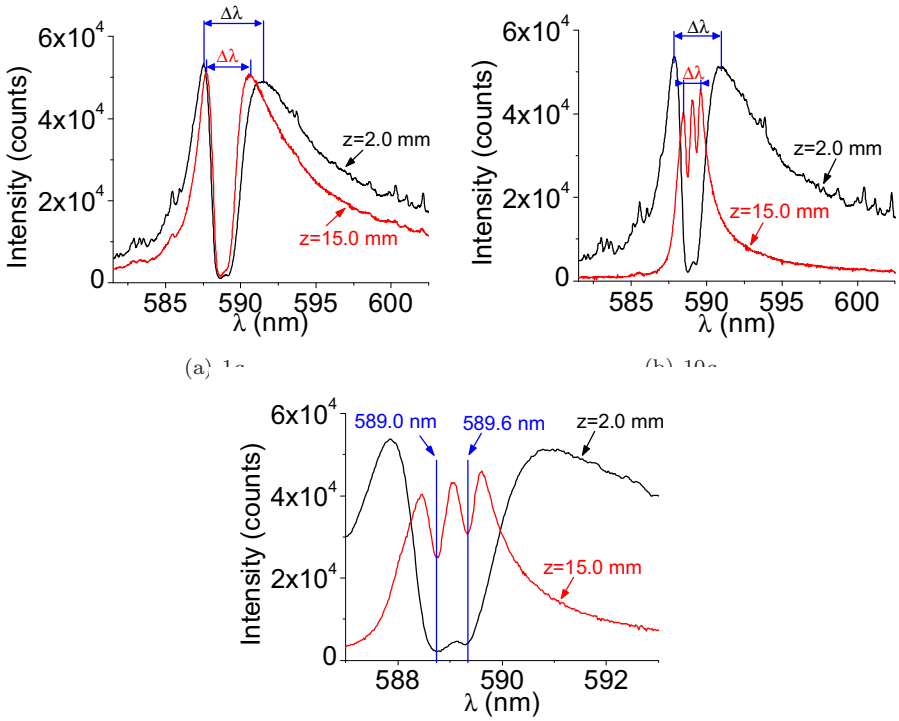

(a) $1g$

(b) $10g$

(c) $10g$, wavelength scale enlarged to view the details of figure (b).

Figure 7.11: Spectra around the Na-D line (589 nm) for lamp C1 (CosmoWhite), 141.6 W, for two axial positions z, at 141.6 W. Closer to the bottom, at $z = 2.0$ mm, $\Delta\lambda$ is larger than at $z = 15.0$ mm, giving a higher NaI density at the wall.

for lamp C1 at 141.6 W, at $1g$, $2g$ and $10g$. From these profiles, we observe that the axial segregation increases when the gravitational acceleration is increased.

Axial intensity inhomogeneity

Figure 7.13 shows the axial intensity profiles for the different emission lines of table 7.2, according to the explanation in section 7.2.3 and figure 7.5. The shape of the Tl curve does not change between $1g$ and $10g$. For the other elements, the shape changes with gravity. The axial density inhomogeneity for the emission lines of different elements (table 7.2) in lamp C1 is shown in figure 7.14(a). The curve for Tl is not shown, because this curve does not change with gravity (figure 7.13). For Hg the inhomogeneity only

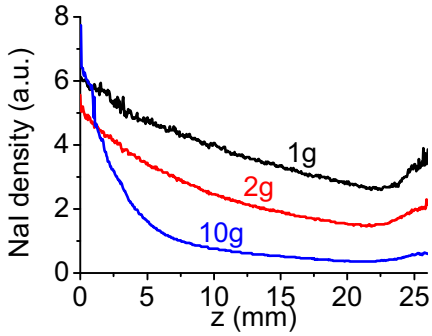

Figure 7.12: NaI density at the wall (equation (7.3)) as a function of the axial position z, for lamp C1 (CosmoWhite), 141.6 W, at $1g$, $2g$ and $10g$.

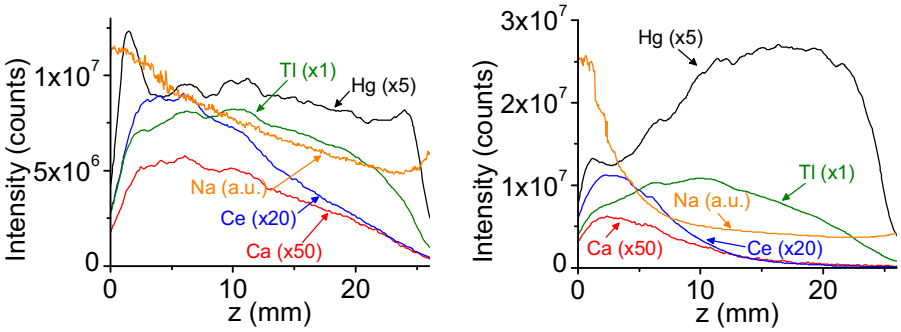

(a) $1g$. (b) $10g$.

Figure 7.13: Axial profiles of Hg 546.07 nm, Ca 442.67 nm, Ce 556.5 nm and Tl 535.05 nm intensities, and NaI wall density (calculated by delta-lambda method in equation (7.3)) for lamp C1 (CosmoWhite) at 141.6 W. The axial position $z = 0$ mm is at the bottom of the lamp and $z = 26$ mm is at the top. The intensity scale is in counts; the measured number of counts for Hg, Ca and Ce have been multiplied by the factors indicated in the graphs. The NaI density is given in arbitrary units.

slightly increases with gravity. For the other elements (Ca, Ce, Na) the axial intensity inhomogeneity increases with increasing gravity. This means that we are at the left-hand side of the Fischer curve (figure 7.1), with the lowest inhomogeneity at $1g$. This confirms that commercial lamps are optimized for use under $1g$ conditions. The Ca inhomogeneity at 100.7 W shows a wiggle, because of the low intensity of this peak.

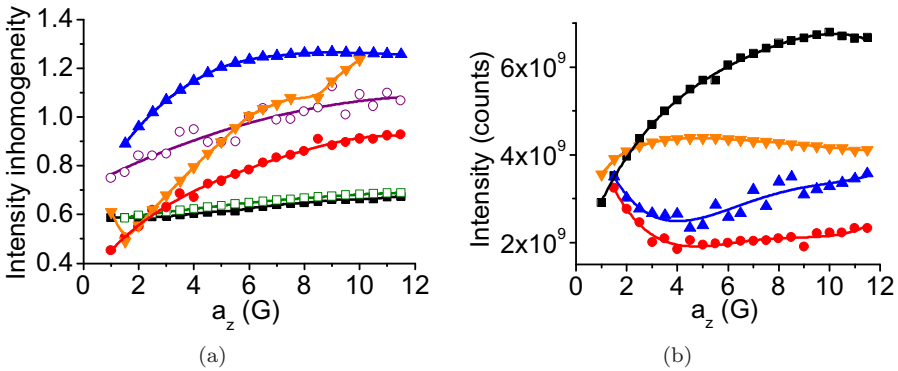

Figure 7.14: (a) Axial intensity inhomogeneity α (equation (7.1)) for different emission peaks for lamp C1 (CosmoWhite), as a function of the gravitational acceleration a_z: ■ Hg 546.07 nm, 141.6 W; □ Hg 546.07 nm, 100.7 W; ● Ca 442.67 nm, 141.6 W; ○ Ca 442.67 nm, 100.7 W; ▲ Ce 556.5 nm, 141.6 W; ▼ Na 589 nm, 141.6 W.
(b) Axially integrated intensity for different peaks for lamp C1 (CosmoWhite), 141.6 W, as a function of the gravitational acceleration a_z: ■ Hg 546.07 nm (values have been multiplied by 3); ● Ca 442.67 nm (values have been multiplied by 80); ▲ Ce 556.5 nm (values have been multiplied by 30); ▼ Tl 535.05 nm (original values).

Axially integrated intensity

Figure 7.14(b) shows the peak intensities as a function of the gravitational acceleration for lamp C1, for Hg, Ca, Ce and Tl. The values for the intensity inhomogeneity of the additives of Ca, Ce and Na get larger when increasing the gravity; the additive densities decrease when going from the bottom to the top of the lamp. Towards the top the additives radiate less; this is compensated by increasing the radiation by Hg.

Temperature calculations

The temperature has been calculated for lamp C1, using the 435.83 and 546.07 nm Hg peaks, according to equation (7.4). Figure 7.15(a) shows the axial temperature profiles at $1g$, $2g$ and $10g$. The temperature observed in the graph is around 3000 K, which is lower than the ∼6000 K one would expect for MH lamps [29, 34, 38, 41]. Therefore, the temperature calculation method as described in section 7.3.3 can be used to obtain qualitative temperature profiles only.[1] The curves show an increasing temperature T as a function of increasing axial position z. The steep increase at the first 2 mm is

[1] A possible reason for the low temperature is scattering of the light by the PCA burner: not only light from the centre is observed, but also scattered light of other regions of the lamp, giving a lower temperature. A second reason is the limited spectral resolution and experimentally observed line width, which makes it hard to resolve the self-reversed Hg lines.

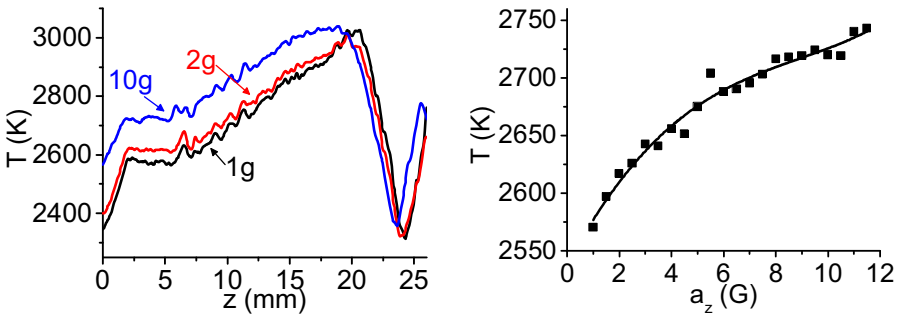

(a) (b)

Figure 7.15: Temperature calculated from the Hg peaks at 435.83 and 546.07 nm (equation (7.4)) of lamp C1 (CosmoWhite), 141.6 W. The temperature is lower than the ∼6000 K one would expect for MH lamps [29, 34, 38, 41]. Therefore, the temperature should be regarded in qualitative terms only.
(a) Temperature profiles for $1g$, $2g$ and $10g$, as a function of the axial position z ($z = 0$ mm is at the bottom of the lamp and $z = 26$ mm is at the top);
(b) Temperature at the axial position $z = 5.0$ mm, as a function of the gravitational acceleration a_z.

caused by electrode effects, also the part above 20 mm is influenced by the electrode. Furthermore the temperature curve moves about 1 mm downwards at $10g$ compared with $1g$. This is caused by the lamp burner that is pulled downward by the large gravitational acceleration.

The temperature for lamp C1 at $z = 5$ mm, as a function of the gravitational acceleration, is shown in figure 7.15(b). The temperature increases with increasing gravitational acceleration. This is explained by the larger axial intensity inhomogeneity of the additives, when increasing the gravitational acceleration. Less additives in the arc means that the radiation comes from the Hg in the lamp, and for radiation by Hg a higher temperature is needed.

The results show a non-uniform axis temperature, which was the reason to introduce the axial intensity inhomogeneity parameter α (sections 7.3.1 and 5.3.3, where the non-uniform axis temperature was obtained by numerical modelling).

7.5 Conclusions

MH lamps have been measured by means of emission spectroscopy. A centrifuge was used to vary the gravity between $1g$ and $10g$. The emission spectroscopy presented in this chapter is an additional method to ILAS and ALI, which are accurate techniques to measure absolute number densities and temperature profiles in the lamps. The

emission spectroscopy method is a fast and easy method to determine the non-uniform axial distribution of radiating particles in the lamp.

We verified the method of emission spectroscopy. We therefore first investigated MH lamps containing Hg and DyI_3 as salt additive. The values for the axial intensity inhomogeneity of Dy are similar to those obtained by ILAS in chapter 6 [72]. ILAS is limited to a fixed salt filling (DyI_3) and geometry. Lamps with a short, wide burner and with a long, thin burner have also been measured. The short, wide lamps show that we are more at the left in the Fischer curve. This is in agreement with the ILAS measurements. For the long, thin lamps, we are at the right-hand side of the Fischer curve, which is in agreement with ALI measurements [38].

From these results obtained for lamps with DyI_3, we conclude that the emission spectroscopy method can be used to characterize MH lamps. This allows us to characterize commercial lamps, such as the Philips MASTER CosmoWhite. We presented the axial inhomogeneity of the different additives (Ca, Ce, Tl, Na). In addition, the NaI density at the wall was derived for these lamps. We also derived the temperature for these lamps. However, the obtained temperature is too low ($\sim$3000 K) compared with what one would expect ($\sim$6000 K), so the claim in literature [82] that this method derives the temperature in quantitative terms, is not valid for our lamp and setup. The discrepancy is most probably caused by the limited resolution of our setup. Therefore, we use the obtained values only for qualitative purposes.

For all lamps, the axially integrated intensities were shown. In addition, we showed some spectra of the lamps. The intensity of the additives is the highest at $1g$ for all lamps. Furthermore, for the CosmoWhite lamp the axial intensity inhomogeneity is the smallest at $1g$, showing that this lamp is optimized for use at $1g$.

In conclusion, the emission spectroscopy in this chapter is an easy and fast method to investigate MH lamps, including commercial lamps like the Philips MASTER CosmoWhite.

Acknowledgements

The authors are grateful to all participants in the ARGES project for their contributions, especially the General Technical Department of the Eindhoven University of Technology for building the centrifuge, to Philips Advanced Development Lighting, and Senter-Novem (project EDI 03146), SRON [66] and the Dutch Ministries of Research and Education as well as Economic Affairs for funding the research.